A Preliminary Study of the Locking of an Interferometer for Gravitational Wave Detection

B.Caron[a], A.Dominjon[b], C.Drezen[b], R.Flaminio[b], X.Grave[b], R.Hermel[b], F.Marion[b], L.Massonnet[b], C.Mehmel[a], R.Morand[b], B.Mours[b], V.Sannibale[b], M.Yvert[b]

[a] *LAMII, BP 806,F-74016 Annecy CEDEX, France*

[b] *LAPP, BP 110, F-74941 Annecy-le-Vieux CEDEX, France*

Abstract

Large interferometers aiming at the detection of gravitational waves are under construction. They use multiple optical cavities and require a coherent control of several mirror positions without spoiling the detector sensitivity. In the case of the VIRGO interferometer several solutions to this problem are currently under study inside the collaboration. In this paper we describe a preliminary study of one of these solutions. We discuss the sensitivity of the controlled interferometer and present some tests done through a simulation of the apparatus. The limitations of the presented solution are discussed.

LAPP-EXP-96.04

Submitted to Astroparticle Physics

1 Introduction

The VIRGO gravitational wave detector will be a Michelson interferometer with 3 km long arms. The experiment is supported by the CNRS (France) and the INFN (Italy). Its construction is under way and the detector shoud be ready in year 2000. The interferometer will contain Fabry-Perot cavities in the arms and the light will be recycled. The layout of the detector has been described in details elsewhere [1, 2]. Figure 1 sketches its optical configuration. The mirrors are suspended masses to be seismically isolated. The suspended mirrors oscillate around their equilibrium points at very low frequency with an amplitude of some tens of the light wavelength λ. However, to reach a working point for the interferometer, the distances between the mirrors must be fixed within a range as tight as a few $10^{-6}\lambda$ for some of them: the Fabry-Perot cavities and the recycling cavity must be kept at resonance with respect to the laser source and the output of the interferometer must be a dark fringe. There will be local damping systems to reduce the amplitude of the mirror oscillations down to a fraction of the wavelength, which is not sufficient to meet the required precision. A higher level control system is thus necessary to lock the interferometer, and this will be achieved in VIRGO with digital servoloops using global information. Such a system has to reduce the low frequency motion of the mirrors without affecting the interferometer sensitivity in the detection bandwidth. Expressed in the usual h unit giving the relative arm length variation, the design sensitivity is $h = 10^{-21}/\sqrt{\mathrm{Hz}}$ at 10 Hz and 3 $10^{-23}/\sqrt{\mathrm{Hz}}$ at 100 Hz.

In this paper we investigate one of the possible strategies for this control system and study its influence on the signal detection as well as its limitations. We begin in section two by giving some general considerations on the control scheme and on the sensitivity of the controlled interferometer. Section three is then devoted to simulation tests. After a short description of the models used in the simulation we examine the performance of the system with a particular choice of feedback. The limitations due to the dynamic range of the signals flowing in the servoloops are then addressed, as well as the issue of the system robustness.

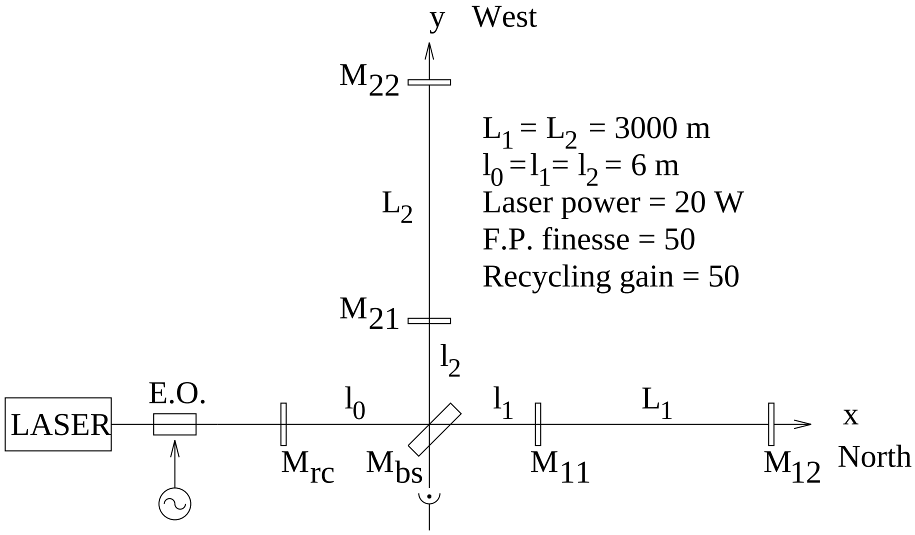

Figure 1: Sketch of the optical configuration of the VIRGO interferometer.

2 Sensitivity of the controlled interferometer

Four independent lengths of the interferometer must be controlled (see figure 1): the lengths of the two Fabry-Perot cavities (L_1 and L_2), the length of the recycling cavity ($l_0 + (l_1 +$

$l_2)/2$) and the arm length difference of the short Michelson ($l_1 - l_2$). As a consequence, four independent error signals must be extracted. This will be done using a technique of high frequency phase modulation-demodulation of the laser light - such a technique being already needed to extract the gravitational wave signal in a frequency domain free of laser power noise. Various modulation configurations have been proposed and studied [4]; some of them have been considered in the case of VIRGO (external modulation, simple frontal modulation, single side band frontal modulation) [3, 5, 6]. The study we report here was done in the case of a simple frontal modulation scheme.

In this configuration, many signals collected from photodiodes situated at various places in the interferometer can be considered to extract the desired error signals. It has been shown [6] that four independent signals can be obtained using the following set: in phase signals of photodiodes d_1 and d_2, and both in phase and in quadrature signals of photodiode d_5 (see figure 2). Let us stress that although these signals are independent, they are not decoupled, all of them depending on all the relevant lengths. There is indeed a natural coupling of the information relative to the lengths of the two Fabry-Perot cavities due to the recycling cavity. Moreover, most photodiode signals are sensitive to variations of the short distances (l_1, l_2) in the same way as to variations of the long distances (L_1, L_2) apart from a finesse factor. The usual method in such cases consists in trying to extract error signals as decoupled as possible to feed back each of them to a single mirror. In this paper we propose a different method by considering globally the set of error signals and taking into account the couplings [7].

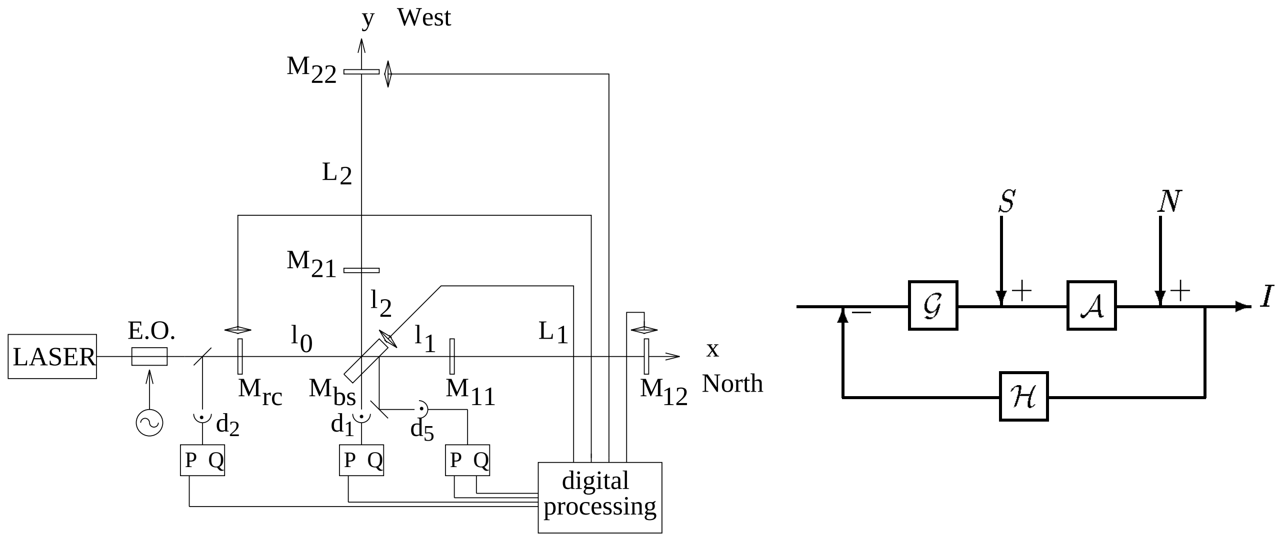

Figure 2: A possible scheme for the control of the VIRGO interferometer (left). Block diagram of the controlled interferometer (right).

Considering the six mirrors of the interferometer, the high level control system will maintain the positions of four of them with respect to the positions of the other two which will have local controls only. The block diagram of the globally controlled interferometer is shown on figure 2, with the following notations:

- $\mathcal{G}$ represents the open loop mechanical transfer function of the interferometer. Since we are considering a set of four identical suspensions and mirrors, we have $\mathcal{G} = G\,\mathcal{I}$ with $\mathcal{I}$ the order four identity matrix and G the transfer function for one mirror. G is a pendulum-like second order transfer function between the applied force and the longitudinal displacement of the mirror.

- S is a four vector containing the displacements of the free mirrors due to external excitations such as gravitational waves, seismic noise or thermal noise.
- A is a four by four matrix relating the longitudinal displacements of the four mirrors (relative to the position of the free mirrors) to the four vector containing the noise free signals collected on the photodiodes. This matrix represents the optical transfer function of the interferometer.
- N is a four vector containing the value of the noise (shot noise and electronic noise) for each photodiode signal.
- I is the four vector of photodiode signals: I_1, I_2, I_{5p}, I_{5q}.
- $\mathcal{H}$ is a four by four matrix relating the vector of error signals to the vector of forces fed back to the mirrors. The choice of a strategy for the control system lies in the choice of $\mathcal{H}$.

When the loop is open we have:

$$I = \mathcal{A}\ S + N \tag{1}$$

The best sensitivity to a gravitational wave excitation is of course obtained on the dark fringe signal I_1:

$$I_1 = \mathcal{A}_{1j}\ S_j + N_1 \tag{2}$$

When the loop is closed we have:

$$\begin{aligned} I &= \mathcal{A}\ S + N - \mathcal{AGH}\ I & (3)\\ I &= (\mathcal{I} + \mathcal{AGH})^{-1}\ (\mathcal{A}\ S + N) & (4) \end{aligned}$$

If one keeps considering I_1 when the loop is closed, the sensitivity seems to be degraded since the noises from the other diodes are now contributing to I_1 through the term $(1 + \mathcal{AGH})^{-1}\ N$. However if one assumes that the loop gain $\mathcal{AGH}$ is known, it is possible to reconstruct the quantity $((1 + \mathcal{AGH})I)_1 = \mathcal{A}_{1j}\ S_j + N_1$ which exhibits the same sensitivity as open loop I_1.

This recovery of the sensitivity relies on the knowledge of $\mathcal{AGH}$. Since we use digital filtering, $\mathcal{H}$ should be known with good accuracy whereas the knowlegde of $\mathcal{AG}$ (which represents the overall mechanical and optical transfer function of the interferometer) demands a good understanding of the experimental setup associated with reliable simulation possibilities. Experimentally, valuable information for the signal reconstruction will be derived from a calibration procedure monitoring slow variations in the response of the detector to known excitations of the mirrors. In the end the sensitivity issue turns into a robustness issue since one has now to consider to what extent imperfections in the loop gain knowledge are tolerable to preserve the system stability and sensitivity.

3 Simulation

In this section we describe some tests of a particular control strategy performed using a simulation of the detector. The simulation approach allows to integrate mechanical, optical and electronic aspects.

3.1 Models

Mechanical simulation

A complete suspension chain of a mirror consists - from top to bottom - of the following elements: a movable suspension point, a chain of seven seismic filters and a positioning device - called marionetta - suspending the mirror and its reference mass [2, 1]. The simulation of the mechanical behaviour of this complex setup is based on a numerical integration of the differential equations describing the movement in one dimension of a chain of massive pendula. The equations take into account the acceleration transmitted to the suspension point due to ground motion as well as the force applied on the mirror from the reference mass. The value of the seismic excitation is computed randomly according to a frequency spectrum in $1/\nu^2$ and its amplitude is tuned so as to obtain the desired range of motion for the mirror taking into account the effect of the active damping systems of the suspension which are not simulated explicitely. The model includes also the pendular thermal noise of the mirror.

The time step chosen for the numerical integration of the mechanical equations corresponds to a sampling frequency of 10 kHz and is compatible with the fastest pole of the closed loop system. Figure 3 shows the distribution of the simulated mirror position when the loop is open. The distribution exhibits a RMS value around 2.5μm, which is a conservative starting point since it is about a factor of three larger than what is expected from the performance of the whole - locally controlled - suspension [1].

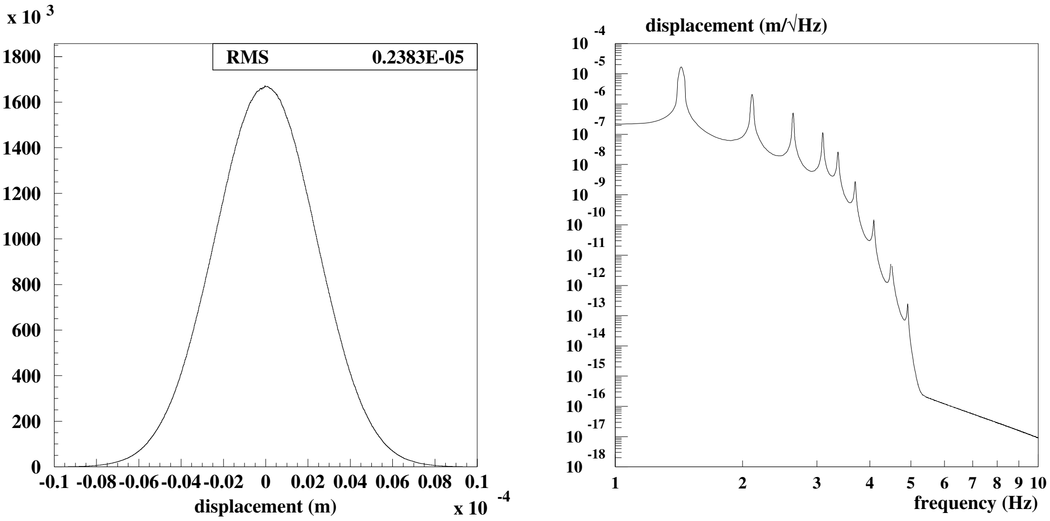

Figure 3: Displacement distribution (a) and spectral density (b) of a free suspended mirror around its equilibrium point.

Optical simulation

The simulation of the interferometer response to movements of the mirrors relies on an analytical calculation [6] which has provided the relationship - in the linear and quasistatic regime - between variations of the characteristic lengths of the interferometer and the signals seen at the modulation frequency by the relevant photodiodes. As mentioned above the study is done in a simple frontal modulation scheme and the considered signals are the in phase signals of photodiodes d_1 and d_2, and both in phase and in quadrature signals of photodiode d_5. The optical model provides in the end values for the elements of matrix $\mathcal{A}$. We assume that the elements can be considered to be independent of frequency (quasistatic approximation), which may be a crude approximation since the bandwidth of the considered servoloops is around

100 Hz. A detailed analysis of the frequency dependence of the elements of matrix $\mathcal{A}$ will be the subject of further study, as well as the consequences on the feedback system.

Integration

Integrating the simulation of both the mechanical and the optical response of the interferometer, we perform a simulation in the time domain of the controlled apparatus. At each time step the positions along the beam of all the mirrors are computed, the corresponding signals collected by the photodiodes at the modulation frequency are derived. These signals are used as position error signals in the recurrent equations associated with the compensators $\mathcal{H}$ (derived from the analytical form using the impulse invariance method) to compute the forces fed back to the mirrors at the next time step. We get information on the system behaviour in the frequency domain by performing FFT's of the time sequences thus obtained.

Four mirrors of the interferometer have to be controlled to lock the interferometer; we have chosen to act on the recycling mirror, the beam splitter and the end mirrors of the Fabry-Perot cavities, the front mirrors of the Fabry-Perot cavities being left free. Therefore all the displacements of the controlled mirrors are computed relatively to the positions of the two free mirrors.

In this study we are concerned only with the linear regime of the feedback system; we do not address the issue of lock acquisition. An easy way to stay away from the non linearities associated with the lock acquisition phase - from a simulation point of view - is to initiate the simulations starting from mirrors at rest and this is what has been done in all the simulations reported here.

3.2 Choice of $\mathcal{H}$

We have shown that the system sensitivity does not depend on a particular choice for $\mathcal{H}$. There is therefore a lot of freedom in the choice of $\mathcal{H}$, which can be made in terms of simplicity and specification matching. Simplicity suggests to decouple the error signals, that is to say to take $\mathcal{H}$ of the form $\mathcal{H} = \mathcal{K}\mathcal{B}$ where $\mathcal{B}$ is the four by four matrix inverse of matrix $\mathcal{A}$. In this case $\mathcal{B}I$ is a four vector containing the decoupled error signals relative to each of the four controlled mirrors and the four by four matrix $\mathcal{K}$ can be taken to be a diagonal matrix of four independent compensators, one per mirror.

Further simplicity can be obtained by using the same compensator for all the mirrors. The choice of the compensator is then guided by the specifications on the tolerable residual displacements at low frequency. These specifications are best expressed by considering the lengths directly relevant to the resonance and dark fringe conditions, namely L_1, L_2, L_r and ΔL with $L_r = l_0 + [(l_1 + l_2) + F(L_1 + L_2)]/2$ and $\Delta L = (l_1 - l_2) + F(L_1 - L_2)$, where F is a finesse factor: $F = 2\mathcal{F}/\pi$ with $\mathcal{F}$ the finesse of the Fabry-Perot cavities. The tolerable RMS variations of these lenghts are given in table 1. They were derived requiring that the cavity lengths be kept within a tenth of an Airy peak HWHM and that the sensitivity be not affected by laser power fluctuations of $dP/P = 10^{-8}/\sqrt{\mathrm{Hz}}$. Clearly we need a high gain ($\sim 10^6$) at low frequency, whereas the bandwidth sould be kept limited to avoid problems arising from the dynamics of the interferometer optical response.

In this study we have used a compensator of the form:

$$K = P\frac{(s+a)(s+b)(s+c)(s+d)}{s^2(s+e)(s+f)(s+g)} \tag{5}$$

Length $(F = \frac{2\mathcal{F}}{\pi})$	RMS of residual variation $(\lambda = 10^{-6}$ m$)$
L_1, L_2	$5.10^{-4}\lambda$
$L_r = l_0 + [(l_1 + l_2) + F(L_1 + L_2)]/2$	$4.10^{-5}\lambda$
$\Delta L = (l_1 - l_2) + F(L_1 - L_2)$	$10^{-4}\lambda$

Table 1: Requirements on the stability of the relevant interferometer lengths (F is a finesse factor: $F = 2\mathcal{F}/\pi$ with $\mathcal{F}$ the finesse of the Fabry-Perot cavities).

where s is the Laplce variable and K refers here to any of the diagonal elements of matrix $\mathcal{K}$. We have chosen the values of the coefficents such that the roots and poles of K be the following:

$$\text{roots of } K \text{ (in rad.s}^{-1}\text{)} \begin{cases} -15. \pm 37.\ i \\ -25. \pm 10.\ i \end{cases}$$

$$\text{poles of } K \text{ (in rad.s}^{-1}\text{)} \begin{cases} 0.\ \text{(double)} \\ -6.2832 \\ -550. \pm 500\ i \end{cases}$$

The open loop gain P has been set to 2.24 10^9 kg s^{-3}. Moreover G has the following poles:

$$\text{poles of } G \text{ (in rad.s}^{-1}\text{)} \ -3.7415\ 10^{-6} \pm 3.741657\ i$$

The chosen coefficients lead to the following approximated values of the closed loop poles of the system:

$$\text{roots of } 1 + \text{GK (in rad.s}^{-1}\text{)} \begin{cases} -461.5 \pm 402.7\ i \\ -74.06 \\ -23.83 \pm 49.68\ i \\ -30.76 \pm 12.24\ i \end{cases}$$

Figure 4 and 5 show the shape of the characteristic functions of the system : modulus and phase of the open loop transfer function GK, and modulus of the sensitivity function $(1 + GK)^{-1}$ (which represents the attenuation factor of the loop). The unity gain frequency of the system is 22.2 Hz, the phase margin 45.5°.

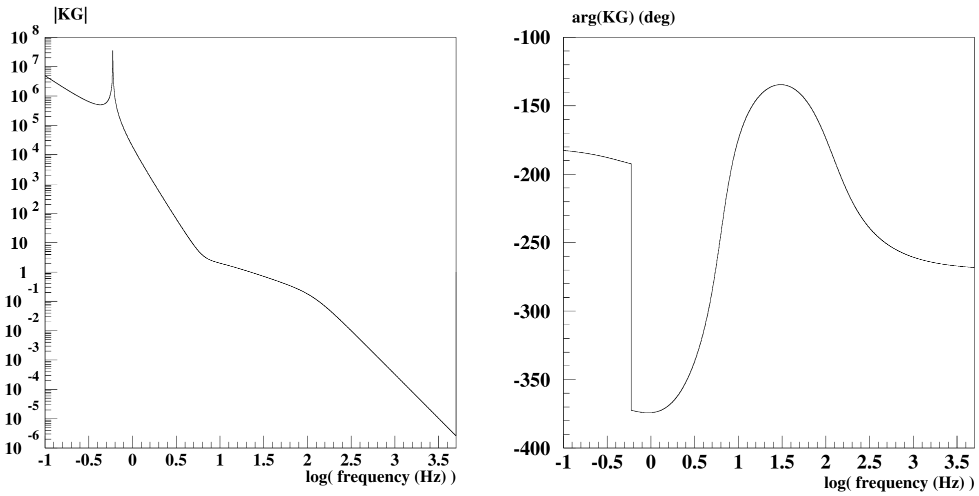

Figure 4: Modulus (a) and phase (b) of the system open loop transfer function $|KG|$. The unity gain frequency is 22.2 Hz, the phase margin 45.5°.

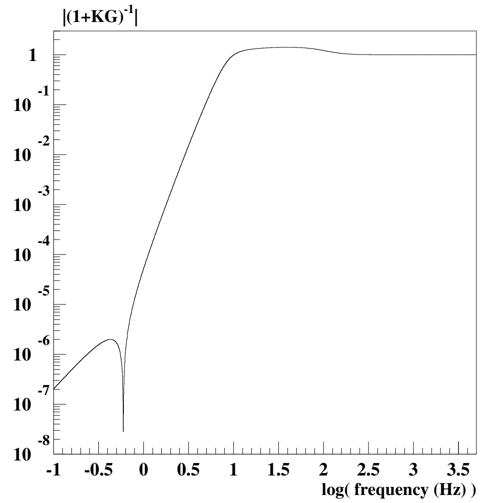

Figure 5: Modulus of the system sensitivity function $(1 + GK)^{-1}$.

3.3 Performances

We evaluate the performances of this tentative control system by comparing the residual motion of the mirrors with the requirements. Figure 6 shows the distribution of the relevant lengths of the interferometer. Comparison with the specifications quoted in table 1 shows that adequate control is achieved, with a sizeable safety factor for L_1 and L_2 (Fabry-Perot resonance consitions), but with no safety factor for L_r and ΔL (recycling cavity resonance and dark fringe conditions). (There is however a small safety factor if we consider that the free RMS displacement of the mirrors has been tuned to a value larger than what is expected.)

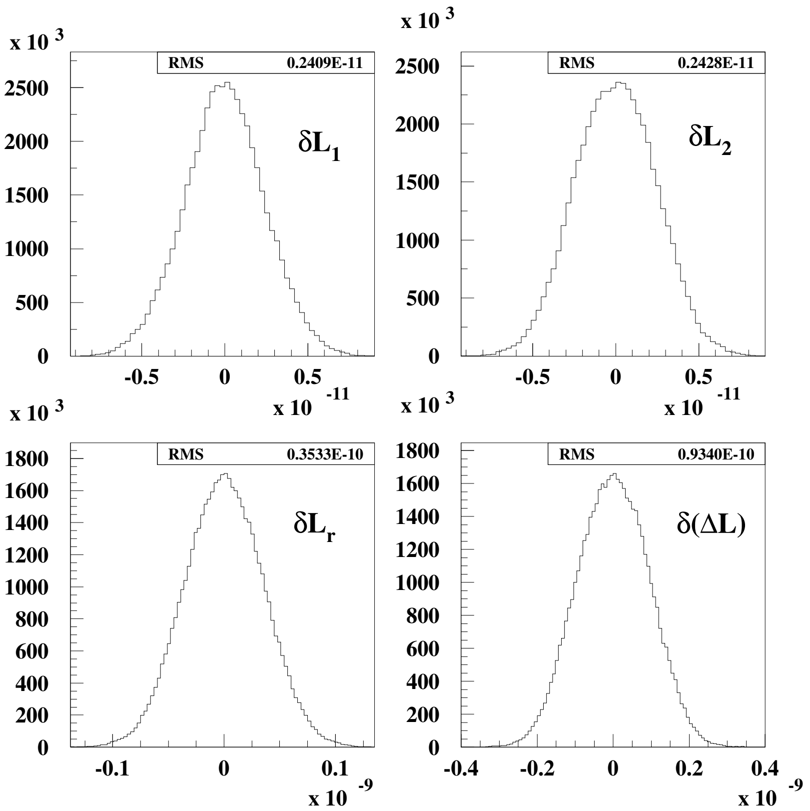

Figure 6: Residual variation distributions of the relevant lengths of the interferometer.

Figure 7 shows the spectrum of the main signal, or dark fringe signal, namely the in phase signal collected on photodiode d_1, and refered to as I_1. Both the spectrum obtained when the loop is open and when the loop is closed are shown, as well as the ratio between the two, which coincides as expected with the sensitivity function of the system (see figure 5).

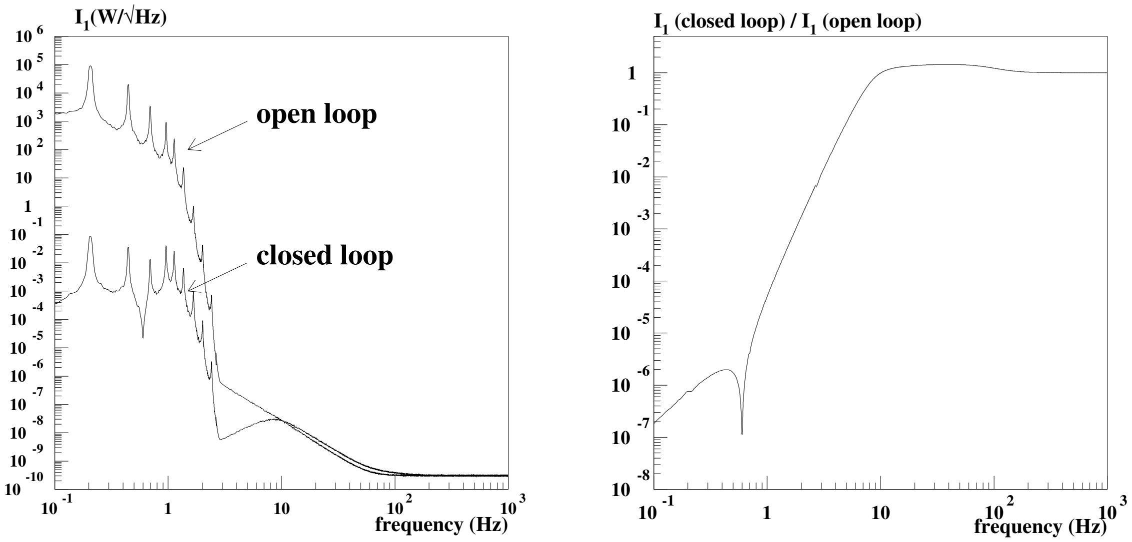

Figure 7: Spectral density of the open loop and closed loop dark fringe signals (a) and ratio of the closed loop spectrum to the open loop spectrum (b).

To extract the sensitivity of the system we can measure the response function to a gravitational wave signal when the loop is closed by applying an excitation on the mirrors in a G.W. like way, as will be done online through the calibration procedure. Measuring the resultant signal I_1 comparatively to the excitation amplitude - expressed in h - as a function of frequency provides the response function shown in figure 8. Dividing the noise spectrum of I_1 obtained when the loop is closed by the response function leads to the sensitivity curve shown also on figure 8.

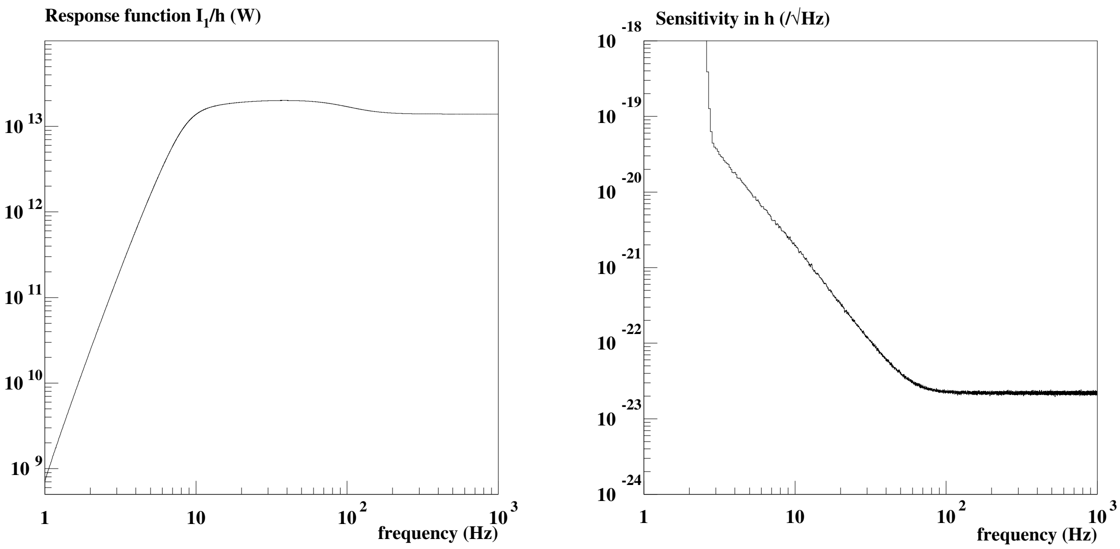

Figure 8: (a) Response of the system as a function of frequency, obtained by applying a white spectrum of calibration forces on the mirrors and measuring the dark fringe signal produced, relatively to the amplitude of the excitation expressend in h. (b) Sensitivity in h of the system, obtained by dividing the spectral density of the closed loop dark fringe signal by the system response function.

The requirement of table 1 on the residual variation of ΔL was derived assuming a level of $10^{-8}/\sqrt{\mathrm{Hz}}$ for the laser power fluctuations. One can check the system sensitivity to the stabilization level of the laser by simulating random power fluctuations using a simple model of white noise. Figure 9 shows the closed loop spectrum of the dark fringe signal when power fluctuations of relative amplitude $dP/P = 10^{-7}/\sqrt{\mathrm{Hz}}$ have been included in the simulation, as compared to the reference spectrum ($dP/P = 0$). The extra noise contribution is clearly visible. Also shown is the ratio of the degraded spectrum to the reference one both for $dP/P = 10^{-7}/\sqrt{\mathrm{Hz}}$ and for $dP/P = 10^{-8}/\sqrt{\mathrm{Hz}}$. One can check that the sensitivity to the stabilization level of the laser is consistent with the performances achieved by the control.

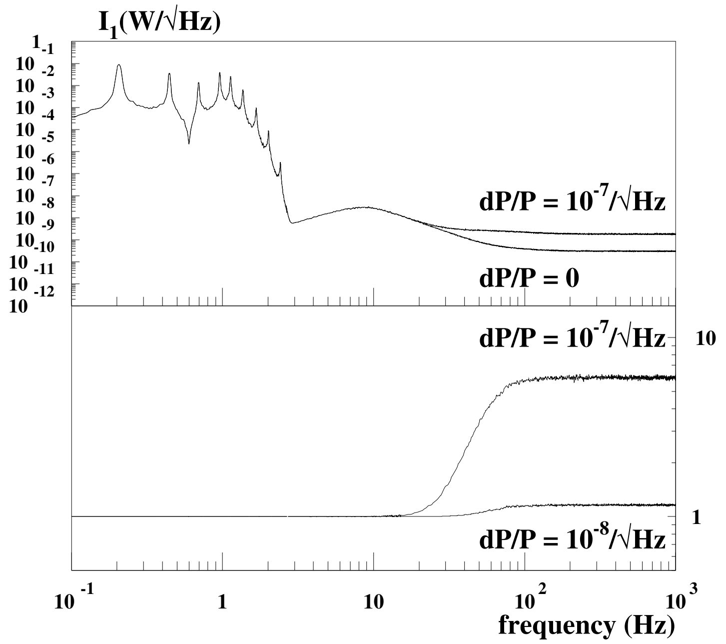

Figure 9: Top: Spectrum of the dark fringe signal with laser power fluctuations, compared to the reference spectrum. Bottom: Ratio of the degraded spectrum to the reference one ($dP/P = 0$) for various levels of laser power stabilization.

3.4 Dynamic range of servoloop signals

In this section we address the issue of the dynamic range of the error signals (photodiode signals) and of the forces fed back to the mirrors. The problems are slightly different in the two cases. As far as the photodiode signals are concerned, the range is limited by the ADC's used in the readout system which in this case can be split into two main channels: a channel dedicated to the locking system, and another one dedicated to the signal detection (see figure 10). This configuration allows to spread the range of the signals over the two channels: the "locking channel" does not need to be shot noise sensitive and needs only to have a range compatible with the feedback system whereas on the "detection channel" the very low frequency part of the signal spectrum can be filtered to restrict the range to that of the signal in the detection bandwidth. In the case of the forces fed back to the mirrors, a unique channel (including a DAC and an actuator) has to be able to stand the whole dynamic range.

We first focus on the error signals used by the servoloops. The needed range is found by simulating the presence in the loops of ADC's of varying precision and looking at the consequences on the signals used for the detection. Figure 11 shows the spectrum of the dark fringe signal when 16 bit or 18 bit ADC's are used - at 10 kHz - in the servoloops. It shows also

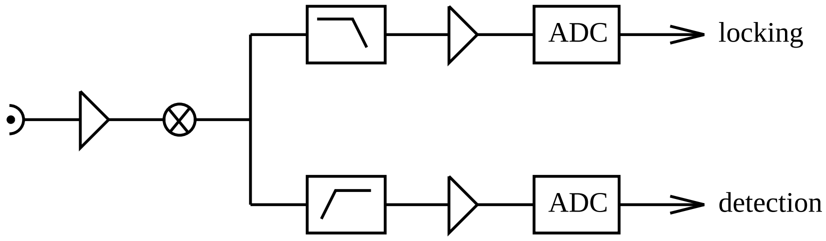

Figure 10: Sketch of a possible configuration for the photodiode readout.

the ratio of the spectrum to the reference one in the case of 18 bit and 20 bit ADC's. The effect of the digitization noise injected in the loops becomes negligible for ranges in excess of 20 bits at 10 kHz, which can hardly be reached by over-sampling an 18 bit ADC. An alternative and promising solution might be to use only one ADC channel and make its precision frequency dependent by using a couple of inverse filters before and after the ADC as sketched in figure 12. The feasability of such a solution has to be investigated.

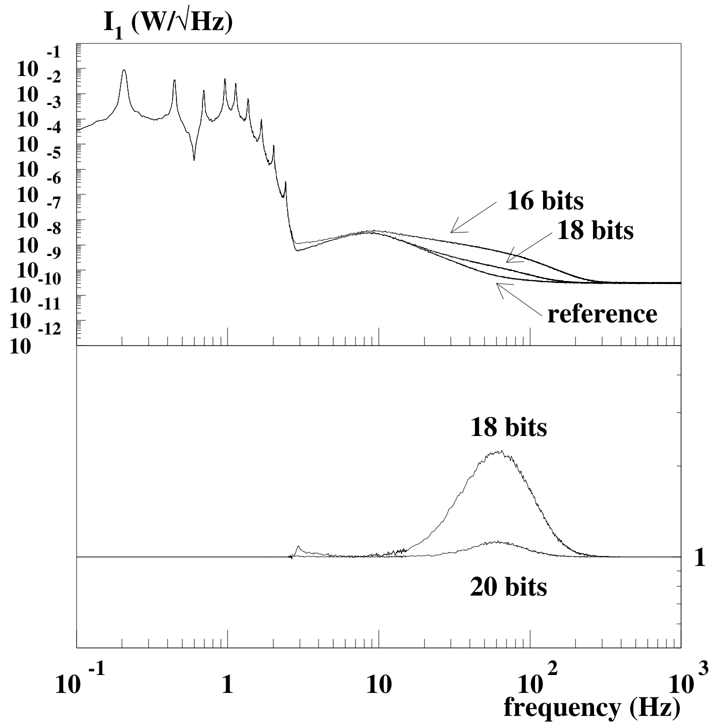

Figure 11: Top: Spectrum of the dark fringe signal when ADC's of various precision are simulated in the servoloops, compared to the reference spectrum. Bottom: Ratio of the degraded spectrum to the reference one for various levels of digitization precision.

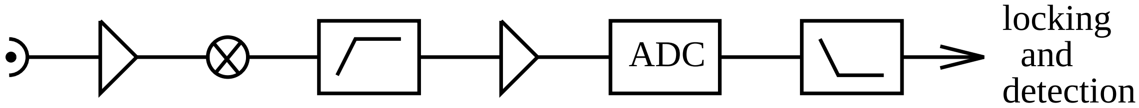

Figure 12: Sketch of an alternative configuration for the photodiode readout.

The problem is even more serious when one looks at the range of the forces fed back to the mirrors. Similar tests show that the actuating device should be able to deliver forces of $10^{-2}N$ while introducing a noise less than $10^{-13}N/\sqrt{\mathrm{Hz}}$ at high frequency, which is far beyond the capacities of either the DAC's or coils involved in the actuating chain. A solution to this problem might be to act on the mirror using not only the actuators situated on the reference mass but also using the marionetta, which would allow to reduce the range of the signals to be sent on each of the two channels. Such a solution raises other problems, in particular concerning stability, and its study is beyond the scope of this paper which deals with a feedback configuration using only the reference mass. Clearly dynamic range issues are a severe limitation to such a configuration.

3.5 Robustness

The key point of the method discussed in this paper lies in the fact that although the different photodiode signals used in the control system are coupled, the sensitivity of the dark fringe signal is not affected by the locking procedure - provided the open loop function of the system is well known. In this section we try to evaluate how precise this knowledge has to be for the sensitivity to be effectively preserved.

In the simulation tests described here we have chosen a particular configuration where we decouple the four servoloops associated to the four controlled mirrors. We adress now the issue of the needed precision for the decoupling operation, namely we study the influence of variations of matrix $\mathcal{A}$ elements, resulting in a matrix $\mathcal{A}^{-1}$ not being exactly equal to the matrix $\mathcal{B}$ used in the digital processing to decouple the error signals.

For the sake of the discussion we now give more details about the matrix $\mathcal{A}$ used in this study. $\mathcal{A}$ can be factorized as $\mathcal{A} = \mathcal{A}_o\mathcal{A}_g$ where $\mathcal{A}_g$ is the matrix relating the mirror displacements to the set of canonical distance variations ($\delta(L_1+L_2)$, $\delta(L_1-L_2)$, $\delta(l_0+(l_1+l_2)/2)$, $\delta(l_1-l_2)$) and $\mathcal{A}_o$ the matrix relating the distance variations to the phtotodiode signals. The elements of $\mathcal{A}_g$ are fixed by the geometry while those of $\mathcal{A}_o$ represent the optical response of the interferometer and are more likely to fluctuate. Therefore we concentrate on the influence of variations of matrix $\mathcal{A}_o$ elements. Their numerical values are given below. They are of course parameter dependent, but for the presence of zero elements which is related to the nature of the beams seen by the various photodiodes and is more general. We have:

$$\begin{pmatrix} I_1 \\ I_2 \\ I_{5\ \mathrm{p}} \\ I_{5\ \mathrm{q}} \end{pmatrix}_W = \frac{1}{2\ 10^{-12}} \begin{pmatrix} 0 & 9.3\ 10^{-3} & 0 & 3.813\ 10^{-4} \\ 6.1\ 10^{-4} & 0 & 2.562\ 10^{-5} & 0 \\ 8.7\ 10^{-4} & 8.6989\ 10^{-6} & -1.914\ 10^{-5} & 0 \\ 0 & 1.5184\ 10^{-7} & 0 & 2.871\ 10^{-6} \end{pmatrix} \begin{pmatrix} \delta(L_1+L_2) \\ \delta(L_1-L_2) \\ \delta(l_0+(l_1+l_2)/2) \\ \delta(l_1-l_2) \end{pmatrix}_m$$

As a first test we evaluate the influence of changing the value of each of the non-zero elements individually. Rewriting I_1 as $I_1 = (\mathcal{A}\ S + N - GK\ \mathcal{A}_o\mathcal{B}_o\ I)_1 = (\mathcal{A}\ S)_1 + N_1 - GK\ \sum_{jk} \mathcal{A}_{o_{1j}}\mathcal{B}_{o_{jk}} I_k$, we can notice that if the first line elements of $\mathcal{A}_o$ are such that $\mathcal{A}_{o_{1j}} = \mathcal{B}^{-1}_{o_{jk}}$ then one recovers the simple expression $I_1 = (1+GK)^{-1}[(\mathcal{A}\ S)_1 + N_1]$. Therefore we expect that only variations of the first line elements of $\mathcal{A}_o$ will have an influence on I_1 (either by a change of the noise level due to contributions from the other diodes or by a change of the loop gain). We observe indeed with the simulation that the elements of the second, third and fourth line of the matrix can be changed within a range determined only by the stability of the system. The allowed range is quite different for one element or another. Systematic tests have shown that the elements can be - individually - changed at least within the following ranges:

$\mathcal{A}_{o_{21}}$	$\times 0. \longrightarrow \times 15.$
$\mathcal{A}_{o_{23}}$	$\times 0.2 \longrightarrow \times 5.$

$\mathcal{A}_{o_{31}}$	$\times 0.5 \longrightarrow \times 5.$
$\mathcal{A}_{o_{32}}$	$\times 0. \longrightarrow \times 10^5$
$\mathcal{A}_{o_{33}}$	$\times 0. \longrightarrow \times 20.$
$\mathcal{A}_{o_{42}}$	$\times 0. \longrightarrow \times 100.$
$\mathcal{A}_{o_{44}}$	$\times 0.5 \longrightarrow \times 5.$

Variations of the first line elements are found to have an impact on I_1 as expected. We have to distinguish two effects: the variation of the loop gain, which if slow enough can be corrected for by measuring the response function of the system through a calibration procedure, and the increase of the noise level due to the contamination from the other diodes which affects directly the sensitivity and cannot be corrected for. To determine the allowed variation range for the first line elements we define arbitrarily an upper limit of 1.5 for the increase factor of the noise spectral density on I_1 at any frequency, after performing calibration corrections. We find that both $\mathcal{A}_{o_{12}}$ and $\mathcal{A}_{o_{14}}$ can be varied within $\pm$ 5%.

$\mathcal{A}_{o_{12}}$	$\pm$ 5 %
$\mathcal{A}_{o_{14}}$	$\pm$ 5 %

Variations of matrix $\mathcal{A}_o$ elements from experimental origin are not expected to occur independently on the various elements but on the contrary with some correlations. A systematic study of all possible correlated fluctuations would be difficult and we consider here only a couple of possible cases. As a first example, a fluctuation in the gain of a photodiode readout channel is expected to result in a scaling factor for a line of $\mathcal{A}_o$. Again, scaling of the second, third or fourth line is allowed within the limit of stability. It is also the case for the first line since a global scaling factor can be completely corrected for by calibration and has no influence on the noise level of I_1. The stability domain has been found to include the following range:

all lines	$\times 0.5 \longrightarrow \times 5.$

In the same spirit and though not directly related to $\mathcal{A}_o$ elements, we can consider the influence of gain fluctuations in the mirrors actuating chains. The recycling mirror actuator is found to have no influence - within the stability domain - whereas the actuators of the other mirrors have to be stable within the following ranges (after calibration corrections and to meet the same criterion as defined above):

Recycling mirror	$\times 0.5 \longrightarrow \times 5.$
End Fabry-Perot mirrors	$\pm$ 10 %
Beam splitter	$\pm$ 5 %

Photodiode d_5 is particuliar since one has to use both the signals in phase and in quadrature collected on this photodiode. An offset in the reference phase used in the demodulation results in a mixing of the third and fourth lines of matrix $\mathcal{A}_o$. The system is found to be quite robust with respect to such an offset since it does not become unstable unless the offset exceeds 40°. In the same way the phase difference between the phase and quadrature components can be increased by as much as 60° before the system becomes unstable.

It is also interesting to evaluate the robustness of the system with respect to delays in the servoloops. From the value of the system phase margin we expect unstability to occur for delays around 10 ms, which has been checked with the simulation. Delays of 5 ms leave the system stable but induce a strong perturbation of the loop transfer function which can be corrected for if the delays are stable enough to allow for calibration. If we consider random delays, then they should be less than 2 ms to meet the already defined criterion.

Let us stress that all the limits given in this section have to be taken separately and are expected to be more severe if several effects are to be considered together.

4 Conclusion

We have presented a preliminary study of a possible solution for the locking of the VIRGO interferometer. We have investigated the possibility of using decoupled servoloops to control the position of the various mirrors. General considerations show that the control might be active in the detector bandwidth without degrading the sensitivity to gravitational wave signals provided a good knowledge of the loop gain and consequently a good knowledge of the interferometer mechanical and optical transfer functions.

Some tests performed through a simulation of the interferometer confirm the expected characteristics of such a solution. The method is found to have some robustness with respect to imperfections in the knowledge of the loop gain and its most severe limitations turn out to be the dynamic range of the signals flowing through the servoloops, especially the ranges of the forces fed back to the mirrors which exceed the capacities of a single actuator. The possibility of a combined control using two different actuators has to be considered.

The simulation of the optical response of the interferometer uses a strong approximation by considering that the matrix relating the distance variations to the photodiode signals is independent of frequency. The elements of this matrix are actually frequency dependent, in a way that has to be scrutinized as well as the consequences on the control.

Besides, other strategies can be envisaged and are currently under study inside the collaboration.

Acknowledgements

We would like to thank our VIRGO colleagues for very useful discussions.

References

[1] VIRGO Coll., Final Design, Version 0 (1995)

[2] VIRGO Coll., Final Conceptual Design (1992)

[3] VIRGO Coll., Proposal for the construction of a large interferometric detector of Gravitational Waves (1990)

[4] R.Weiss, Q.Prog. Rep. Lab. Electron. MIT **105** (1972) 54
A.Billing et al., *J. Phys. E* **12** (1979) 1043
R.W.P.Drever, Gravitational Radiation, les Houches 1982, eds N.Deruelle and T.Piran (North-Holland Amsterdam) (1983) 321
C.N.Man, D.Shoemaker, M.Pham-Tu, D.Dewey, *Phys. Lett.* **A148** (1990) 8
L.Schnupp, Workshop on gravitational wave detectors, Munich (1988)
M.W.Regehr, F.J.Raab, S.E.Whitcomb, *Opt. Lett.* **20** (1995) 1507

[5] C.N.Man, VIRGO note PJT 92 033a (1992)

[6] R.Flaminio, H.Heitmann, VIRGO note PJT 93 021 (1993) and forthcoming publication in *Phys. Lett. A*

[7] B.Bourdas, B.Caron, F.Marion, VIRGO note PJT 95 006 (1995)